Commentary on API RP 1183 – Dent Assessment and Management

B N Leis[1] and A Eshraghi[2]
[1]B N Leis Consultant Inc.
[2]Acuren

Pipeline Pigging and Integrity Management Conference

February 12-16, 2024

Organized by
Clarion Technical Conferences

https://doi.org/10.52202/072781-0004

https://doi.org/10.52202/072781-0004

Abstract

API's release of the first edition of its Recommended Practice (RP) 1183 titled "Assessment and Management of Pipeline Dents" in November 2020, and Errata 1 a few months thereafter, marked the culmination of 14 plus years of related work. Against that backdrop, the PRCI, in collaboration with the PHMSA initiated Project MD-5-1, which sought to assess that activity, to identify technology gaps and aspects of that work that could enhance the RP, or broaden its capabilities. Concurrently, PRCI in collaboration with PHMSA initiated Project MD-5-2 seeking to enhance the tools being adopted in the RP. Aspects of these developments were evaluated rather critically at PPIM2023 in a paper that discussed what it termed "enhancement of indentation crack formation strain estimation" in PRCI's reporting MD-5-2. Independently, about the same time a four-part series of papers was being planned with a similar but much broader intent and complexity, which is now in part in print in a refereed journal. This paper is the practical synthesis of that breadth and complexity, distilled with guidance and with takeaways concerning the issues and limitations of the current RP 1183.

This paper identifies many of the key assumptions latent in the Level 1 and Level 2 practices of API RP 1183, and truth-tests them by comparison with results generated using full-scale-validated Level 3 analyses. Where issues emerged with those assumptions, guidance and takeaways are presented to help mitigate their practical implications. Results for smooth single-peak symmetric and asymmetric dents formed in geometrically stiff versus compliant pipes over a range of depths from less than 1% OD up to 10% OD are considered. It is shown that the Level 1 and 2 practices can be effective for shallow large-radius single-peak dents, as might be formed by smooth rounded field boulders. However, the viability of those Level 1 and 2 practices diminishes as the dent depth and its curvature increase — with major issues emerging at depths as shallow as 1% OD when dealing with smooth flatter asymmetric dents. The RP's concept of dent 'restraint' was truth tested and found problematic at dent depths typical of the shallower populations typically evident in many ILI surveys. The results discussed show that the Level 2 practices of API RP 1183 can underpredict the severity of smooth asymmetric dents by in excess of 100%. Finally, the RP's provisions when dealing with skewed-dents have been truth-tested. For the cases considered it was evident that the peak strain was dictated by the shape of the contact, far more so than by the skew-angle. Because this outcome will be dependent on the shape and size of the dent formed, even low skew-angle dents likely should be evaluated at Level 3. Guidance and takeaways are provided to help manage skewed and other single-peak dents, whereas multipeak dents and those near possibly interacting features are deferred.

Introduction

The first edition of API RP 1183[1] (RP or RP 1183) was released to the public in November 2020, with an Errata issued in January 2021. In association with its release, the API website stated that "The new RP is designed to help maintain the structural integrity of pipelines by addressing mechanical issues. It gives operators the tools needed to help ensure pipeline infrastructure is safe, reliable, and efficient".[2] Given the need for technology to assess damage that would help to ensure that the pipeline infrastructure was safe, reliable, and efficient, it is not a surprise that shortly after its release in-line inspection (ILI) vendors, pipeline operators, and consultants began to assimilate its practices and report on their experiences.[e.g., 3-6] These and other papers like them since tend to follow one of three high-level themes. The first group focuses on the experience developed through implementing and interpreting API RP 1183 in a field setting.[e.g.,3,7,8] The second group considers

https://doi.org/10.52202/072781-0004

the concepts involved and the assumptions that underlie the practices of the RP, and their implications for the validity of its assessments and predictions.[e.g., 9-13] Finally, recognizing that concerns with the practices of API RP 1183 have begun to emerge, a third group is beginning to develop, illustrate, and refine alternative practices.[e.g.,3,14-16]

This paper falls within the framework of the second group, being based on the results developed in a four-part series of comprehensive peer-reviewed papers[10-13], two of which are now in print, while the remaining pair are in press or approaching so. This paper presents a practical synthesis of the breadth and complexity of this four-part series, leading to guidance based on their trends, and takeaways concerning the issues and limitations as of the first errata of API RP 1183 (1st Edition).[1] To avoid the potential complexity of multiple-peak dents, or dents local to coincident / interacting features, this paper focuses on "single-peak smooth dents" as defined in reference to the definitions and terminology used in the RP. While aspects of what follows pertain to the guidance of the RP concerning Level 3, the focus here is on the practices recommended at Level 2 and below.

Some Key Assumptions Embedded in the Practices of API RP 1183

Given the challenge faced by the intent of API RP 1183, its structure and approach must process the output of a deformation-tool survey into a format that can be input to its technology-based dent-severity assessment methods. On this basis there are assumptions latent in the text of the RP that deal with the ILI data-processing aspects directed at extracting required by its tech-based assessment. Likewise, there are assumptions latent in its guidance regarding dent evaluation. Consistent with related API recommended practices, API RP 1183 identifies three levels of analysis, from the simple at Level 1, and the more involved at Level 2, up through the general analysis capabilities at Level 3, which capitalizes on FEA.

This paper focuses on the RP's assessment practices, and by review of its text identifies many of the key assumptions latent in the Level 1 and Level 2 practices of API RP 1183. Thereafter, the paper truth-tests the assumptions specific to the RP's Level 1 and Level 2 practices by direct comparison with results generated using full-scale-validated Level 3 analyses.

Several of the key assumptions inherent in the assessment practices of API RP 1183 follow based on a review of portions of its text and recommendations. This process first considers assumptions relevant to dent geometry and strain analyses during contact and re-rounding, which also are equally relevant to applications that involve fatigue analysis. Thereafter, assumptions specific to the fatigue analysis practices of the RP are identified and discussed.

Section 6.2 of the RP states that "the recommended approach for characterizing a dent involves the development of two-dimensional longitudinal and transverse profiles of the dent shape through the deepest point of the dent". For purposes of integrity analysis it follows that the RP assumes that:

1. the maximum strain develops at and remains located at the apex of the dent; and
2. the highest curvature profiles lie on the transverse and axial planes cut through its apex.

Section 6.2 further states that these profiles are useful to calculate dent strains and a restraint parameter. The practices of the RP smooth the input data as the basis to fit a continuous curve that locally characterizes the shape of the dent. The RP makes reference to an effective strain determined using the strain components as defined by the ASME in Appendix R of B31.8[17]. PRCI Project MD-

https://doi.org/10.52202/072781-0004

5-2[18], which was directed at developing technology to broaden the utility of the RP also makes reference to a somewhat different effective strain that makes use of the ASME bending strain components. It supplements those bending strains with an empirical variation of the ASME axial membrane strain and an adaptation of the transverse membrane strain developed by Gao et al[19]. All such strain components are quantified by curve or other fits to the smoothed dent profiles. As these strain components are evaluated at various endpoints over the deformation and pressure history experienced by the dent, it also follows that the RP implicitly assumes that:

3. the profile-based strain components suffice to quantify the dent's severity, and
4. the effective strain adopted suffices to quantify the plastic-deformation history associated with the dent's formation, re-rounding, and any ensuing cyclic plasticity.

Finally, §6.2 states that "The deepest point of the dent or the dent depth is defined in Figure 7" of the RP. Inspection of Figure 7 indicates that dent depth is defined by the indenter travel beyond the initial point of contact, which is benchmarked therein to a transverse section specific to the undeformed nominal shape of the pipe. Thus, it follows that the RP assumes that:

5. the indentation depth in view of Figure 7 is quantified by reference to the indenter travel relative to the remote undeformed nominal transverse shape of the pipe.

While the indenter travel relative to the remote undeformed nominal transverse shape of the pipe can be measured in physical or numerical experiments, it is unknown in field applications for what the RR terms 'unrestrained' dents, and so must be inferred. That inference could develop by way of Eqn. (1), which empirically correlated the strain based on the field-measured residual dent shape and size to the strain developed during contact, as was detailed in PRCI Project MD-5-2[18]:

$$\epsilon_I = C_1 \times \epsilon_P + C_2 \times \epsilon_P^{|C_3|} \ . \tag{1}$$

Eqn. (1) duplicates Eqn. (4-11) in the just-noted Report, which also indicates that this equation and related work will help to enhance tools in the RP. The symbols $C_i = C_i(OD/t, P_{max}, P_{mean})$, $i = 1,2,3,$ refer to regression coefficients whose values were determined as the best-fit to the FE results; ϵ_P was the effective strain at the dent's apex determined via finite-element analysis (FEA) calculated from the dent's pressure re-rounded profile, and ϵ_I was the dent indentation effective strain. The symbol P_{max} denoted the maximum pressure as a % of the pressure at the specified minimum yield stress (SMYS), which was either incurred in the FEA, or when based on an ILI it quantified the maximum pressure that had been experienced in-service. The symbol P_{mean} denoted the pressure at the time the dent's shape was sized, which also was expressed as a % of SMYS. As the initial effective strain, which derives from Eqn. (1), is the start-point for cycle-by-cycle strain-based fatigue analysis[e.g.20] it follows that viable cycle-by-cycle strain-based fatigue analysis based on the Level 3 practices of the RP must assume

6. Eqn. (1) accurately quantifies ε_I as a function of ϵ_P with minimal uncertainty.

Select assumptions latent in the fatigue analysis practices of the RP follow, the first of which involve discriminating whether a dent is 'restrained' or 'unrestrained', and further whether the dent was 'deep' or 'shallow'. The latter of these was quantified in §8.3.4.1 simply in terms of the host-pipe's diameter as:

- total dent deformation depth < 4 % OD for diameters ≤ 12.75 in. (324 mm), and
- total dent deformation depth < 2.5 % OD larger diameters;

https://doi.org/10.52202/072781-0004

whereas one might anticipate that at least *D/t* also would be a discriminator. Subsection 8.3.4.1 initially considers 1) unrestrained dents and 2) dents there referred as 'deep' restrained dents, with that for 'shallow' restrained dents considered subsequently.

Specific to unrestrained and deep restrained dents §8.3.4.1 states that "the indentation process first flattens the pipe at the indenter contact point then the pipe wall curvature reverses as the dent formation continues." Further, it notes that "the response of dent to internal pressure fluctuations will be different at total dent deformation depths above and below this change in pipe wall curvature". This reversed-curvature occurs during the initial forming of the dent, so the depth of interest occurs at the line-pressure as the dent was being formed. While easy to measure in a test, it can be otherwise problematic. For deep restrained dents this reversed-curvature-depth, herein denoted δ_{RC}, might remain close to that as it was formed. However, such is not so for unrestrained dents — as the ensuing pressure cycles and plastic history can affect the shape of the dent and the pipe local to the dent. Just as ϵ_I in Eqn. (1) was unknown for ILI-based analysis of field dents, the value of δ_{RC} is unknown. Yet, as the process outlined in §8.3.4.1 indicates, and the two points noted in the above paragraph state, the value of δ_{RC} must be known to discriminate whether a dent is 'deep' or 'shallow'. It follows that an equation analogous to Eqn. (1) is essential between analogous displacements denoted δ_{RC} and δ_p to implement the practices of the RP for unrestrained dents. Recognizing that the value of δ_{RC} directly affects the predicted fatigue life for unrestrained dents, this relationship between δ_{RC} and δ_p must be accurate, and lead to minimal scatter, but as yet such an equation has not been reported.

In view of the above it follows that API RP 1183 assumes that:

7. an analog to Eqn. (1) will accurately quantify δ_{RC} with minimal uncertainty.

In lieu of the just-noted analog equation, §8.3.4.1 of the RP makes reference to its Annex G, which presents a dent-shape-based approximation to reflect the influence of δ_{RC} in the form of dent scaling parameters, whose values are presented in a series of tabulations as a function of the service-pressure history and the pressure the dent-shape was measured at (i.e., the local pressure during the ILI run).

Full-scale tests reported in the context of PRCI Projects MD-4-2[21], MD-4-11[22], and MD-4-14[23] as well as numerical studies and trending reported in the context of PRCI Project MD-4-9[24] among others underlie the fatigue analysis practices outlined in §8 of API RP 1183. Fatigue life as characterized in the full-scale testing was reported as total life, which likewise was the case for the RP's life prediction practices. These experiments and analyses considered 'unrestrained' dents, as well as 'restrained' dents. Dent restraint for the purposes of the full-scale tests and their FEA was affected by pressure cycling while not retracting the indenter. Trending of the results from numerical work that considered pressure-cycling of dents for which the indenter was not retracted gave rise to a dent restraint parameter (DRP) whose value was adopted as an indicator of the dent's state of restraint. As §6.4 of the RP details, this DRP was a function of the dent's overall shape expressed in terms of areas and lengths at specific depths based on the characterization of the dent's shape outlined in §6.3. On this basis it follows that the RP assumes:

8. the dent's profile local to its apex conforms to the shape of the indenter, such that presence of the indenter immobilizes the area of the dent under the indenter,
9. the DRP accurately determines dent restraint quantified in binary format termed as generally 'restrained' or 'unrestrained', and
10. restraint can be quantified in terms of the dent's local shape.

https://doi.org/10.52202/072781-0004

The approach adopted in the PRCI reporting makes reference to a single fatigue resistance curve that has its roots in the fatigue of weldments — with BS 7608[25] being cited. Stress-life resistance curves involving weldments[e.g., 26] typically have negative slopes the order of 0.333 or larger[e.g.,27], which is a more negative slope than that observed for resistance curves for failure initiated on surfaces remote to stress raisers. While a single resistance curve was adopted in the work that underlies API RP 1183, it is known that thermal-mechanical and other processing factors can affect order-of magnitude differences in fatigue resistance for similar classes of steel[e.g.,28]. Such resistance variability is apparent for example in Figure 4.5 of the Report for PRCI Project MD-4-14[23]. This figure presents the full-scale test data developed for plain dents made in the four pipe steels considered in the PRCI MD Projects. Inspection of that figure indicates that a negative slope of –0.333 was adopted, which as alluded to above is typical of weldments. In contrast, fatigue resistance curves for plain dents developed in work for the EPRG show shallower negative slopes, the order of –0.231 or less[29]. Shallower resistance curves with slopes like –0.231 versus the –0.333 noted for Figure 4.5 lead to significantly different fatigue lives, which approach a factor of 10 or more on life at longer lives.

Adopting a single fatigue-resistance curve, and using a 'shape parameter' (denoted SP) as done in API RP 1183 to account for the dent's severity, leads to a generic equation to predict the fatigue resistance of a dent, or its fatigue life in cycles to failure, N. In a form analogous to the long-known power-law stress-life (S-N) fatigue curve[30] this leads to an equation with the form:

$$N = A(SP)^b, \tag{2}$$

which is like that of Eqn. (28) in API RP 1183, except that the exponent B here is lower-case by author's preference to remain consistent with the usual format of such equations[31]. In this form, *N* is the number of cycles to failure. On the usual log-log plot of the SP on the y-axis and *N* on the x-axis the value of *A* is determined by the y-intercept at N=1, whereas the value of *b* is determined by the negative slope of the resistance curve. The values of the parameters *A* and *b* uniquely characterize the specific fatigue resistance curve that was adopted in the work of PRCI Project MD-4-9[24], which underlies the RP. With this form, if the shape parameter served its intended function, then it would uniquely quantify the severity of the dent. In turn, dent fatigue resistance would be uniquely quantified by the single pair of the fitting constants *A* and *b* evident in Figure 4.5 of the MD-4-14 Report[23].

The format of Eqn. (2) indicates that API RP 1183 assumes that:

11. the fatigue resistance of all line-pipe steels of interest can for its purposes be quantified by a single resistance curve, and
12. the shape parameter and its embedded consideration of restraint uniquely quantifies the effects of the dent's shape, depth, and formation history, and its restraint, and its service loading for purposes of life prediction.

Finally, consider the influence of skew-angle, which as it can be present for both monotonic and cyclic loading is noted last. Section 8.3.2 states that the Level 1 approach is not applicable to "dents that are oriented at an angle greater than 30° with respect to the longitudinal axis". Section 8.3.4 states that "the same angular limit of 30 degrees shall be applied" in the context of its Level 2 practices. On this basis it follows that the RP assumes that:

13. a skew-angle of 30° reflects a breakpoint in the response of a dent, above which Level 3 practices must be adopted.

https://doi.org/10.52202/072781-0004

Viability of Select Key Assumptions and their Practical Implications

While important assumptions other than those noted above can be identified within the practices of API RP 1183, the above-outlined set of 13 more than suffice to support the scope and intent of this commentary. Whereas some readers might be interested in the implications of these 13 assumptions, others might be interested only in a subset. This observation coupled with the length and scope of a typical PPIM paper constrains what can be considered hereafter in detail. That said, the focus here is limited to the assumptions numbered 1-4, 6, 9, 12, and 13. The first four assumptions are related, and so will be considered in reference to the same dent-pipe combinations. That said, on the surface the last four appear independent of one another, and so are discussed in the above sequence.

Assumptions One to Four

The first assumption — that the maximum strain 'develops at and remains located at the apex' of the dent — appears logical given that this paper only considers smooth single-peak dents. The second and third assumptions follows logically from the first and so also are physically appealing, but dependent on the viability of the first. Quite simply, if there is only one peak, how then can the strain, which for bending relates to curvature, be greater other than at that peak? If it remained that simple as the dent deepened, then 'the highest curvature profiles' could only fall on the transverse and axial planes that were cut through its apex as assumed within the practices of the RP. Finally, the fourth assumption reflects two coupled concerns. First, its outcome depends in part on the viability of first three assumptions. Second, and more critical, is the presumption that a profile-based effective strain evaluated at discrete points in a dent's deformation history suffices to quantify that history.

Issues and Implications

Regarding the first assumption, logic and analysis both make it clear that point-contact occurs when an indenter and a pipe first come together. When shallow, the apex (deepest point) of the dent is in full contact with the impinging surface of the indenter — that is the pipe-wall conforms with the impinging surface (and so shape) of the indenter. However, depending on the stiffness of the pipe (affected by D/t and internal pressure), and the radii of the pipe and the contact, as the depth of the contact increases the contact surface between the pipe and indenter begins to shift out onto the shoulders of the indenter and the re-entrant shoulders of the dent — and the apex begins to unload. If this shift only occurred at larger depths of no practical interest, then for the purposes of RP 1183 it would be of no consequence. For this reason, this paper considers a range of dent depths from very shallow up to just slightly beyond 6% of the outside diameter (OD), which currently is the least restrictive bound on dent depth found in Codes and Regulatory mandates known to the authors (e.g., ASME B31.8[17]). This Code and others[e.g., 32] also include other more restrictive bounds depending on the circumstances local to the dent. In addition, API RP 1183 in regard to 'restrained' dents defines 'shallow' as a depth less than 4% OD for pipe diameters less than 12.75 inches and as less than 2.5% OD for larger pipe diameters. Figure 1 schematically helps to visualize why this shift in dent response occurs, using images that reflect a range of dent depths, pipe stiffnesses, and pipe and contact radii.

The upper row of Figure 1 reflects very stiff (low *D/t*) pipes, while the lower row reflects very compliant (high *D/t*) pipes, with the dents in both rows formed by a slightly increasing moderate contact force, which leads to increasing but very different dent depths, and deformation response local to the dent. The left pair of images represent a small-radius indenter in contact with a much

https://doi.org/10.52202/072781-0004

larger-radius pipe. The central pair considers a somewhat larger-radius indenter in contact with the same pipe. Finally, the right pair are similar, except that the radius of the indenter is now like that or larger than that of the pipe.

Inspection of the left pair of images indicates that little to no dent forms for the stiff (low *D/t*) pipe, whereas a very shallow dent forms for the compliant (high *D/t*) pipe, for which the pipe fully conforms to the indenter. The central pair of images indicates that for this scenario the response is much different. For the stiff (low *D/t*) dent-pipe case the indenter sets up and out on the re-entrant shoulders of the dent, leaving the apex just unloaded. In contrast, as for the left image for the compliant high *D/t* pipe the pipe fully conforms to the impinging surface of the indenter. Finally, as the radius of the indenter becomes large compared to the pipe, their geometries coupled with their stiffnesses result in the contact for both pipes shifting out onto the shoulders of the indenter and the re-entrant shoulders of the dent — forming a gap between them. Figure 2 quantitatively illustrates key aspects of the schematics in Figure 1 by reference to the strain and contact-pressure footprints developed at or approaching the bounding cases across this spectrum of dent-pipe combinations.

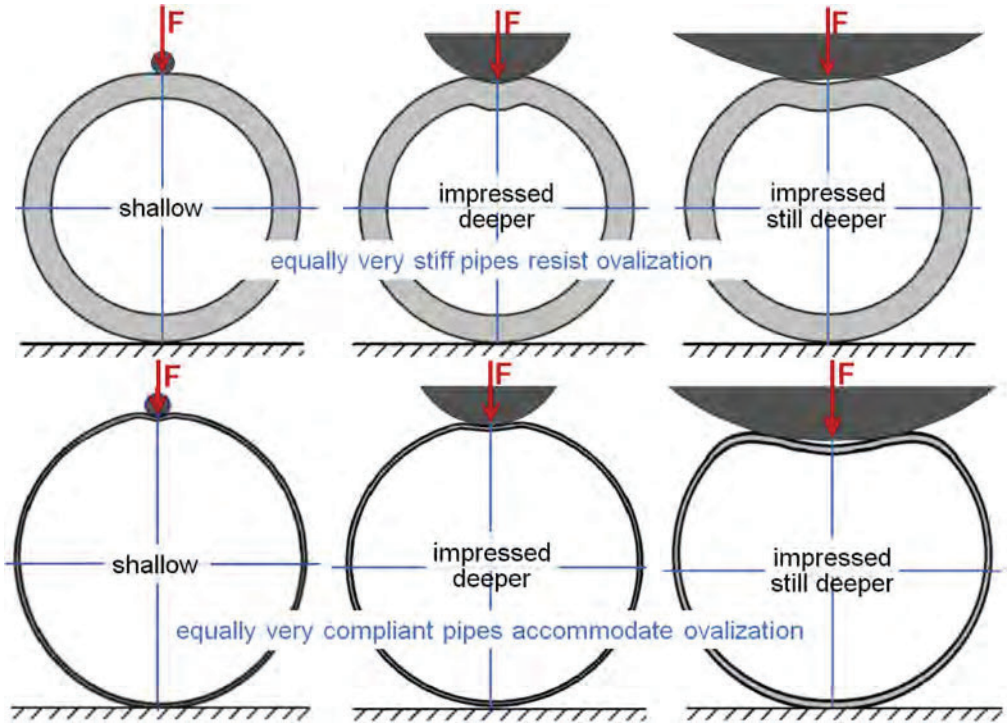

Figure 1. Schematic depicting the dependence of the pipe's response to contact as a function of pipe stiffness (affected by pressure and D/t) and the ratio of the pipe to indenter contact radius

Figure 1 indicates that the two very different dent-pipe combinations shown in its upper-left and lower right corners bound the dent response that could develop in the field. On this basis, it is instructive to consider the response of dent-pipe combinations that tend toward those bounding states, which is done by reference to their equivalent plastic strain and contact pressure (in psi) footprints, as shown in Figure 2. Plastic strains are relevant for present purposes because it is plastic deformation that forms dents and other permanent deformations in pipelines. Whereas a range of dent sizes and shapes are evident in the r,θ,z output from a deformation-tool-run, the majority of the features sized typically have maximum depths less than 3% OD and after processing consistent with API RP 1183 tend to be close to symmetric. To that end Figure 2 characterizes shallower dents.

https://doi.org/10.52202/072781-0004

All images in Figure 2 are oriented with their axial direction horizontal, and all reflect the response at their maximum dent depth. As then their maximum strains lie on the ID surface of the pipe, the strain footprints shown quantify the ID response. But as contact with the indenter occurs on the OD surface of the pipe, the contact-pressure footprints quantify this pressure on the OD surface. The scale of the images included in the upper row, which shows their strain contours, applies equally to the lower row, which shows their contact-pressure footprints. The left-side images in Figure 2 characterize the response for the combination of a smaller-diameter low *D/t* pipe deformed by a very small diameter indenter — which reflects the bounding case that lies in the upper left image in Figure 1. For this case *D/t* = 18, and the ratio of the pipe's radius to the transverse radius of the indenter was very high at about 23. The right-side images in Figure 2 characterize the response for a high *D/t* =96 pipe for which the pipe radius to transverse indenter radius was quite low at about 0.5. This dent-pipe combination reflects the bounding case that lies in the lower right corner in Figure 1.

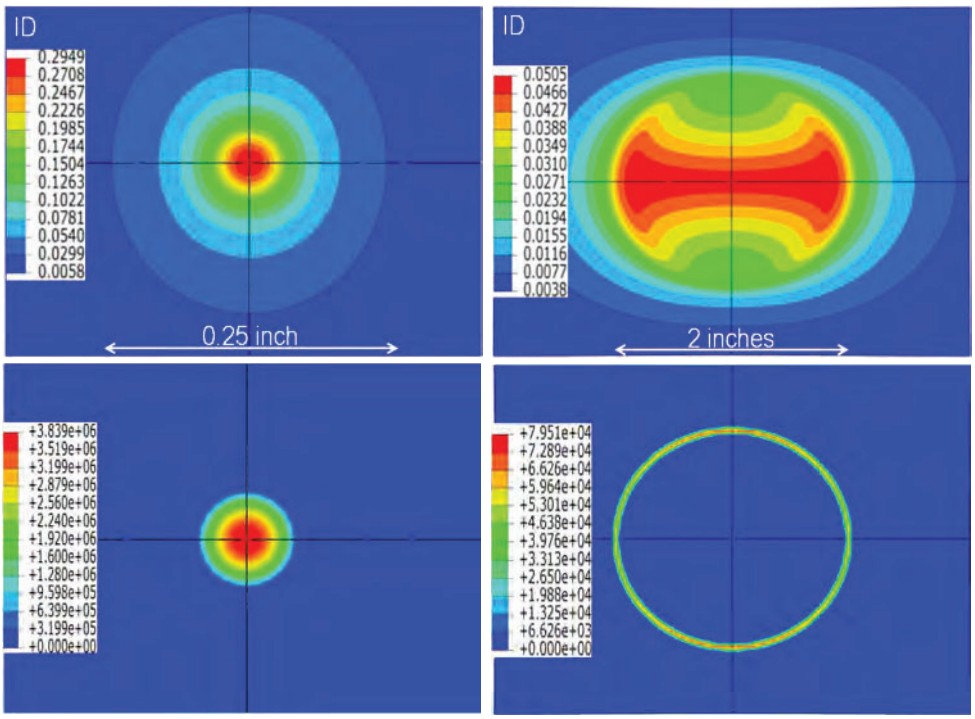

Figure 2. Contrasting the effects of pipe stiffness and ratio of the pipe to indenter radii as evident in their strain and contact-pressure footprints

The response for the low *D/t* pipe was quantified for contact by a smooth hemispherical 0.200-inch diameter indenter with a 4.5-inch diameter Grade X52 pipe with a 0.250-inch-thick wall. Its equivalent plastic strain footprint is shown for contact at P_{mean} equal to 30% of P_{SMYS}, which due to the pipe's high stiffness resulted in a very shallow dent depth of just 0.045 inch (0.89% OD). The corresponding footprint for the larger radii contact relative to the pipe involved a high *D/t* Grade X70 pipe with a diameter of 36-inches and wall thickness of 0.375-inch. The strain footprint shown for this scenario reflects contact at P_{mean} = 10% of P_{SMYS} between a compound hemispherical indenter with a 38.5-inch contact radius. The resulting contact for this more compliant pipe developed a dent depth of 1.08 inch (3% OD).

https://doi.org/10.52202/072781-0004

As would be expected in view of the first of the above-listed API RP 1183 assumptions, the strain and contact footprints for the very small diameter indenter relative that of the low *D/t* pipe were fully symmetric below its re-entrant shoulders. This symmetry and their gradual monotonic increase with depth into the apex indicates that the pipe wall conformed locally to the hemispherical shape of the indenter. Such conformal contact leads to axial and transverse dent profiles that satisfy the first three of the above-listed assumptions of the RP. Thus, the response of this bounding dent-pipe combination confirms the viability of the practices of API RP 1183 for what was a very shallow dent.

In strong contrast, study of the strain footprint for the compliant high *D/t* pipe, whose compliance makes it much easier for it to conform to the indenter, indicates that the response for this dent-pipe combination violates each of the first three assumptions, as follows. While its displacement profile showed a single-peak plain dent whose apex remained located as it was at its initial contact, observe that the nearly symmetric profiles that formed for shallow contact have become orthogonally asymmetric[1] as the dent deepened to a depth of just 3% OD. While the maximum strain has remained on the axial dent profile, a more refined view of the strain distribution shows that its maximum value has shifted axially away from its apex. That refined detail indicates that equivalent plastic strain at the apex was 4.89% whereas the maximum remote to the apex the equivalent plastic strain was 5.2%, for which the corresponding total strain was about 5.4%. The corresponding apex value of the three-component profile-based ASME effective (total) strain[(18)] was 5.2%, while that for the four-component MD-5-2 effective (total) strain[(18)] was similar at 5.52%. In view of the FEA equivalent strain results, due to the migration of the maximum strain away from the apex the strain there is about 6% less than the peak strain. On this basis, the practices of API RP 1183 would underestimate the maximum strain for this dent by about 6%. As the depth deepens this error tends to increase, becoming significantly more nonconservative[(11)].

Key Observations for Later Discussion

Several observations central to the viability of the practices of API RP 1183 follow for later discussion in view of the results for the two dent-pipe combinations considered in Figure 2:

- while the maximum strain initially developed at the dent's apex, it did not remain there but rather migrated well away from the apex — consequently Assumption 1 that "the the maximum strain develops at and remains located at the apex of the dent" is violated — the discussion later illustrates this for cases leading to significant errors in predicted strain;
- while the highest curvature remained on the axial plane cut through its apex, the peak strain was not quantified by the transverse profile cut through its apex — consequently Assumption 2 that "the highest curvature profiles lie on the transverse and axial planes cut through its apex" is violated — the discussion later illustrates this for cases leading to significant errors in predicted strain; and
- the profile-based strain components failed to quantify the dent's peak strain (severity), which violates the expectations of Assumption 3 — the discussion later illustrates this for cases leading to very large errors in predicted strain.

The consequences of violating these assumptions varies depending on the dent-pipe combination considered within the spectrum evident in Figure 1, as discussed briefly in the next subsection.

The Spectrum of Dent-Pipe Deformation Response

[1] Whereas API RP 1183 considers symmetry referenced independently to the axial and transverse planes, as stated in References 10 and 11 symmetry for present purposes is assessed relative to the response below the reentrant shoulders of the dent, and there reflects rotationally (fully) symmetric deformation.

https://doi.org/10.52202/072781-0004

The above discussion concerning the two dent-pipe combinations that bound the response evident in Figure 1 indicated that stiff pipe forms shallower dents because it resists deformation. In contrast, its compliant counterpart when subjected in the field to comparable contact-loading conditions forms deeper dents. As was evident for the D/t = 18 pipe subjected to contact by a much smaller-radius indenter, the dent's shape well below its re-entrant shoulders remained symmetric — and in spite of this lower D/t pipe's stiffness the pipe-wall locally conformed to the indenter. Whereas the compliant pipe-wall would be expected to conform to the shape of its indenter, that did not happen. Rather, it was clear that the resulting dent unloaded at its apex as the contact shifted away from its apex out onto the shoulders of the indenter. The strain distribution responded, developing its peak strains out toward the sites where the contact pressure was most intense.

Inspection of the lower row of images in Figure 2, which quantifies the contract-pressure footprints for these bounding dent-pipe combinations, helps to illustrate and so clarify the very different behavior for this pair of dents. The footprint in the left image, which reflects the response when a dent is shallow, shows that for this hemispherical contact the contact pressure is greatest at the apex of the dent. The contact pressure there is very intense, and correspondingly the strain there is very high (about 29.5%). As expected, given the radiused shape of the indenter, this contact pressure gradually decreases moving away from the apex. On the other hand, the compliant pipe deforms more readily, and as the dent depth increases and its effects spread transversely, the upper-quadrant of the pipe begins to behave like an arch. An arch stiffens as its loading spreads across its span, because its vertical reaction component to that loading becomes dominant. This affects a shift in the contact from local to the apex, out onto the shoulders of the indenter. The contact pressure is correspondingly smaller, and correspondingly so are the strains (the maximum here is about 5%).

Figure 3 illustrates the shift in the location of contact in response to increasing dent depth. To remain relevant to the response of low D/t pipes, this image is specific to dents formed in 8.625-inch diameter low D/t = 26 X52 pipe in contact with a rigid 7-inch diameter hemispherical indenter, which leads to a pipe to indenter radii ratio of 1.23. On this basis this dent-pipe combination lies very near the right margin in the schematic shown in Figure 1, and so reflects this bound's response for low D/t pipes.

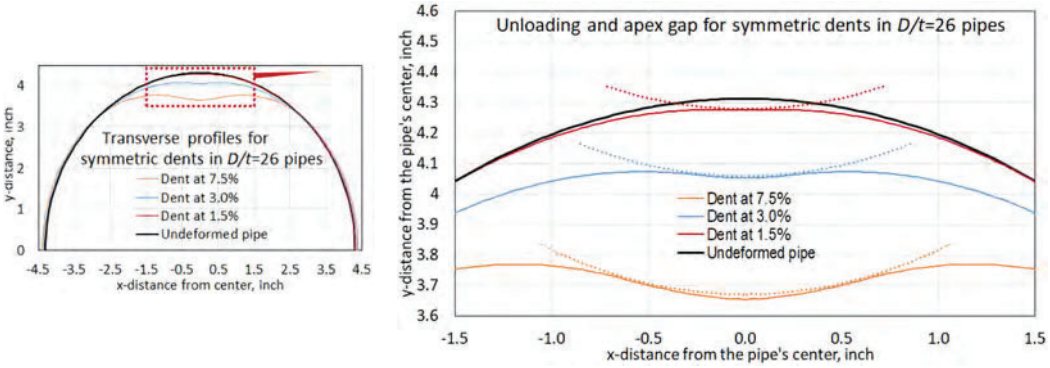

Figure 3. Transverse profiles for a 'restrained' dent, showing a shift in the anulus of contact pressure, and the increasing gap formed as the dent unloads due to increased dent depth[11]

The left image in Figure 3 shows the profiles of three dents over the upper quadrants of the pipe at depths of 1.5, 3.0 and 7.5 %OD. It is evident from this plot that these pipes have increasingly ovalized as the dent depth and the corresponding force required to form the dent increased. As these dents had been formed without internal pressure, these profiles reflect ovalization at its worse for this dent-pipe combination. The right-side image in Figure 3 focuses on these profiles local to the

https://doi.org/10.52202/072781-0004

top of the pipe. Each of these profiles has been overlaid with the shape of the rigid 7-inch-diameter hemispherical indenter that formed them, which has been set just tangent to the pipe. At the image scale practical for this paper the gap that forms between the face of the indenter and the surface of the pipe and the locations of their tangency is clearly evident only for the deepest of these dents. That said, as the dent depth decreases the gap decreases as does the distance between the locations of their tangency.

It is clear from the results of these FEA that the contact between the apex and the indenter is lost for this dent-pipe-pressure combination at a depth between 0.75 and 1.5 %OD, whereafter the surface of the dent subject to unloading continues to expand about the dent's apex. While for stiff pipes the affected area can be small, Figure 2 indicates that for the compliant pipe considered there this unloaded area is about 3 square inches. Logically, larger unloaded areas develop, depending on the dent's shape and profile and the diameter of the pipe. Likewise, the extent of the unloading diminishes as the line pressure is increased — but because the effect of pressure is secondary to that of pipe stiffness the unloading and associated gaps persist at the highest pressures of practical concern.

It follows in view of Figures 1, 2, and 3 that there is a spectrum of dent response that ranges between the two bounding cases considered, which depends on the pipe stiffness (affected by pressure and D/t), and the ratio of the pipe to the indenter's contact radii. Whereas these bounding cases and the schematics in Figure 1 have considered radiused contact, the field reality opens to contact with rocks and earthmoving implements. This adds to this complexity regarding rather than simplify it because the dent's overall shape and profile can be axially as well as transversely asymmetric. Insight into the range of rock geometries that can be encountered becomes evident from the images presented here in Figure 4, which shows rocks representative of those evident along three pipeline construction sites.

Figure 4. Images illustrating rocks in rights-of-way as potential sources of rock dents

The left image in Figure 4 illustrates rocks evident in the windrow of spoil created as the trench was dug or machine cut. The central image is similar, except that it illustrates rocks along the ditch-bottom due to collapse of the cut along either side of the lowered-in pipe string, being captured later in the construction process just prior to bedding and padding this pipe segment. Finally, the right image was taken from above the pipeline segment wherein rocks evident were overlaid in the backfill above the pipe after the crown of the pipe was padded. These images make it clear that rock-dents will form as a result of rounded boulders that could cause nearly symmetric dents. Asymmetric rock shapes and/or the larger flatter rocks and/or rock-ledges would give rise to asymmetric dents, which if angled to the pipeline lead to skewed asymmetric dents. Rocks with angular profiles have the potential to form kinked features. Finally, even what appear to be soft compliant sandbag benches have led to dents in higher D/t construction — leading to asymmetric dents. Topside dents also develop a similar range of dent types, but these are more commonly formed due to outside forces.

https://doi.org/10.52202/072781-0004

Questions for Later Discussion

Given that extensive FEA generated strain results like those reported in Figure 2 underlie the practices of API RP 1183, two questions beg to be asked:

- In that FEA were completed in the work that underlies the RP and for this paper have led to differing observations and implications, can two sets of FEA runs made on comparable commercial platforms solving the same problem generate fundamentally different outcomes? Unfortunately, the answer is YES!
- If unloading occurs leading to zero contact pressure as was clearly evident in Figure 2 and/or the gaps between the indenter and the pipe wall as in Figure 3, then the indenter is not in physical contact with the pipe-wall — absent physical pipe-to-indenter contact an indenter left impressed at its deepest point **cannot** physically 'restrain' the dent's apex — in a full-scale test or a FEA! In this context is a 'restrained dent' as quantified in API RP 1183 and the underlying PRCI reporting a viable concept?

Consideration of these questions and their answers is deferred to the discussion section, which will address these others that emerge for the remaining assumptions examined.

Assumption Six

As outlined earlier, Eqn. (1) empirically correlated the effective strain based on the field-measured residual dent shape and size to the effective strain during contact, as was detailed in PRCI Project MD-5-2[18]. As Eqn. (1) is contemplated for inclusion in API RP 1183, it would be anticipated to accurately quantify ε_I as a function of ε_P with minimal uncertainty. To that end Eqn. (1) was evaluated for symmetric, transversely asymmetric dents, and doubly asymmetric dents over a range of depths from less than ≤ 1% OD up through 10 % OD[10,11]. Of the four scenarios examined in detail for this generic set of dent types, Figure 5 summarizes the results for the two dent-pipe combinations considered, which lay between the least and worst of the errors developed by Eqn. (1). Because the related details are presented elsewhere[10,11], suffice it here to summarize the outcomes in graphical format in Figure 5. Because failure as the dent is being formed is anticipated on the pipe's ID surface, and also is possible there during increasing pressure due to pressure cycling, this error analysis was done in reference to ID strains. Conversely, failure as the contact is retracted is anticipated on the pipe's OD surface, and also possible there during pressure cycling, this error analysis also was done in reference to OD strains. The error in the value of ε_I predicted by Eqn. (1) has been determined relative to a Level 3 FEA analysis using analysis practices and models that have proved valid in reference to full-scale test results detailed in Reference 22. The mesh for that validation and all others considered made use of an element size sufficiently refined for each dent-pipe combination considered.

The benchmark for each error analysis was the corresponding FEA-determined equivalent plastic strain. As usual for such error analyses, the error is defined as the difference between the benchmark and the predicted values divided by the benchmark, which then is multiplied by 100 if the error is to be expressed as a percentage. This result is plotted on the y-axes in Figure 5, wherein each image makes use of a different scale to accommodate the trends evident. As defined, positive values are conservative, whereas negative values are nonconservative. The many data points evident in each plot reflect the form of the correlation that underlies Eqn. (1) and the practices of the RP and related PRCI reporting. As indicated earlier, the constants C_i in Eqn. (1) depend on the *OD/t* for the dent-pipe combination considered, and the maximum pressure incurred either in the FEA, or experienced in-service, earlier denoted P_{max} as well as the pressure at the time the dent was sized in the ILI, earlier

https://doi.org/10.52202/072781-0004

denoted P_{mean}. The values of P_{max} for the two dent-pipe combinations considered are shown on the x-axes in Figure 5, which consistent with the practices of the RP ranged from 20% to 80% of the specified minimum yield stress (SMYS).

Each of these scenarios was evaluated across a range of values of P_{mean} consistent with the scope evident in the practices of the RP. This analysis scope leads to 45 FEA runs per dent depth. On this basis the data shown for the six depths considered in the upper-pair of images in Figure 5 involved a total of 270 FEA runs. These results, which lie toward the larger of the predicted errors, quantify the errors in the predicted response of fully symmetric dents in depths from 1% to 10% OD. As one fewer dent depths were considered for the results shown in the lower-pair of images in Figure 5, this dataset required a total of 225 FEA runs. These results, which lie toward the lesser of the predicted errors, quantify the errors in the predicted response for doubly asymmetric dents in depths from 1% to 5% OD.

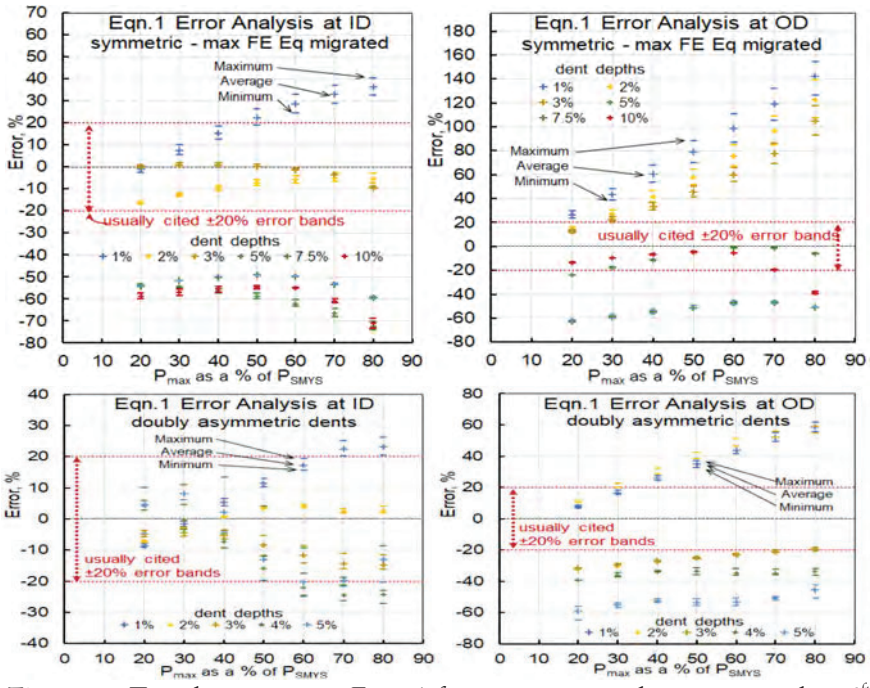

Figure 5. Trending errors in Eqn. 1 for symmetric and asymmetric dents[after (11)]

Inspection of the data trends summarized in Figure 5 shows that the predictions of Eqn. (1) can err ranging from positive and in excess of 150% to the other extreme — unconservative and approaching –80%. Further it is evident that there is no simple pattern in the size or sign of the errors, which could reflect the differing effects of pipe stiffness (D/t and pressure) and dent depth on the location of the contact patch and pressure. Rather surprisingly, the error developed for the asymmetric dent in this case was less than that for the symmetric dent. But as this error can be strongly affected by the unloading of the dent's apex, this will not always be the case.

An Issue and its Implications for Later Discussion

Suffice it in view of Figure 5 to conclude that as formulated and calibrated Eqn. (1) is an inconsistent predictor that is prone to very large errors. Its positive errors will drive unnecessary / valueless digs whereas its unconservative errors pose a risk of potential failure.

Assumption Nine

https://doi.org/10.52202/072781-0004

While conceptually independent of the above discussion, the assumption that the dent's profile local to its apex conforms to the shape of the indenter, such that presence of the indenter immobilizes the area of the dent under the indenter, is violated for reasons evident in view of the five assumptions discussed above. Figure 2 showed complete unloading at a dent's apex that was evident with zero contact pressure over an area of 3-squeare-inches. Unloading at the apex to a contact pressure of zero was broadly evident in the results presented in Reference 11, which in some cases had expanded over an area of about 15 square-inches. The gap between the indenter and the pipe wall as in Figure 3 begs the question — absent pipe-to-indenter contact how can an indenter left impressed at its deepest point physically 'restrain' the dent's apex — whether in a full-scale test or in a FEA?

An Issue and a Related Question for Later Discussion

Suffice it in view of Figures 2 and 3, and similar behavior broadly evident even for dents as shallow as 1%, to ask: how absent physical pipe-to-indenter contact an indenter left impressed at its deepest point can physically 'restrain' the dent's apex? In turn this begs the question: is the concept of a 'restrained dent' as quantified in API RP 1183 and the underlying PRCI reporting viable?

Assumption Twelve

The shape parameter (SP) that is central to this assumption is equally central to the fatigue life prediction scheme adopted in API RP 1183. Three related facts are key in this context, as follows.

- First, as Assumption 11 makes clear, the fatigue prediction practice detailed in the RP makes use of a single fatigue resistance curve[e.g., see 22]. This curve was in the form of the usual 'S–N' stress whose roots lay in BS 7608[25] (recall that earlier S denoted stress, while life in cycles was denoted, N).
- Second, fatigue life in the format of a 'S–N' curve[2] as quantified by Eqn. (28) depends on the stress cycle, ΔS, and the mean stress, S_M, local to the site where cracking initiates. Figure 6 presents the simulated fatigue life based on values of SP calculated in Level 3 PRCI-CEPA FEA. There the predicted values of N are shown on the logarithmic y-axis as a function of the corresponding values of SP that are shown along the logarithmic x-axis. As has been broadly documented for more than 70 years[e.g.,35], the mean stress has a first-order effect on fatigue life, which varies dependent on ΔS. On this basis, all factors that affect ΔS and S_M equally affect the fatigue life.
- Third, the form of the RP's Eqn. (28) that relates fatigue life to the SP dictates that the predicted fatigue life depends solely on the SP. In turn, this dictates that the value of the SP must correctly embed the many factors that affect the fatigue failure of a dent.

[2] It became clear beginning about the late 1950s that the utility of a curve that quantified fatigue life in the format of a 'S–N' curve was limited to 'longer' fatigue lives, because of the effects of yielding. Longer in this context is quantified by the so-called transition fatigue life[e.g.,20], which for steels often lies between 1,000 and 10,000 cycles to failure.

https://doi.org/10.52202/072781-0004

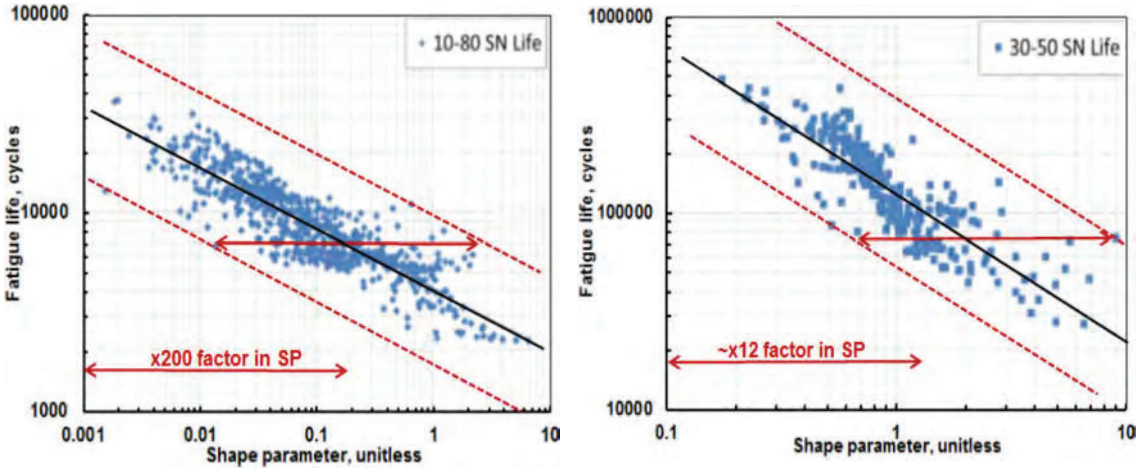

Figure 6. Fatigue life as a function of the SP

Given that viable life predictions require that the value of the shape parameter account for the many factors that control the values ΔS and S_M, it follows that viable fatigue-life predictions at a dent must consider at least:

i) restraint to the extent it actually developed local to the origin of the cracking;

ii) its shape and size, including that local to the origin of the cracking, as these affect the local cyclic stresses (and strains), and the local mean stress;

iii) its formation history, as this can have a first-order effect on the cyclic stress range and the mean stress; and

iv) its service history, which must reflect ΔS and S_M over the potential life of the dent.

The challenge posed by expressing the fatigue life, N, in the form N = f(SP) as in the practices of API RP 1183 becomes evident as discussed by Dinovitzer et al[34] in regard to Figure 6. In reference to Figure 6 and Reference 34, each datapoint represents a unique FEA run specific to the dent-pipe combination considered, and the deformation and pressure history for which a value of the SP was determined, with the life, N, then determined by the single S-N curve adopted for use in RP 1183. On this basis, if the values of the shape parameter correctly quantified the parameters controlling the fatigue life, then all predicted lives (i.e., each datapoint) would fall along a straight-line trend in such figures, and the scatter would disappear! It is, however, clear from Figure 6 that such is not the case. The left image in Figure 6 reflects the resulting scatter for 'unrestrained' dents that were subject to constant amplitude pressure cycling from 10% to 80% of SMYS. As highlighted in these images, the model-error implicit in the SP is large, as its value varies for the same fatigue life by a factor as large as 200. The outcome for 'restrained' dents subject to similar pressure cycling but from 30% to 50% of SMYS as evident in the right image in Figure 6 is not as bad, but it reflects far fewer FEA cases.

An Issue and its Implication for Later Discussion

The tabulations in Annex F of the RP list values for the constants in Eqn. (28) of API RP 1183 (or Eqn. (2) as shown earlier) that attempt to offset its model-error circa 2014[33]. It is however evident that after this empirical 'fix' a scatter-band for the SP of about 200-fold persists (e.g., see Figure 5-10

https://doi.org/10.52202/072781-0004

in Dinovitzer et al[34]). On this basis, the model-error embedded in the shape parameter remains large. Consequently, as formulated in the RP the outcomes predicted in regard to the SP will remain scattered. Moreover, the related trending is benchmarked to the central tendency within the scatter, some predictions will remain very conservative while others will be equally unconservative. This will continue until the complexity embedded in the dent's deformation history is addressed, and the uncertainty embedded in its approach to 'restraint' is resolved.

Unfortunately, the dent's reshaping as it deforms and its contact pressure distribution evolves opens to its apex unloading, and its maximum strain's migration, neither of which can be captured within the approximations that underlie API RP 1183 — except at strains below which this behavior occurs. In turn, this limits the utility of its practices to rather shallow dents.

Assumption Thirteen

Assumption 13 addresses the role of skew-angle relative to the longitudinal (long) axis of the pipe as outlined in the RP. The practices of the RP discriminate between skewed dents specific to a skew-angle of 30°[3], and recommend that dents with skew-angles larger than 30° be assessed at Level 3, whereas those with lesser angles can be assessed at a lower level. As all dents save for fully symmetric dents can be formed skewed to the pipe's long axis, this recommendation has been assessed specific to skew-angles of 0°, -5°, +5°, +25°, +45° – each of which formed a smooth single-peak but still rather flat doubly asymmetric dent with an indentation depth of 5% OD. That said, given the outcomes[11], similar conclusions would be drawn for many other dent-types and geometries.

Figure 7 evaluates the dependence of the maximum -equivalent plastic strains that developed on the ID and OD surfaces of the above-noted five dents[11]. This peak strain is plotted on the y-axis versus the skew angle and ID versus OD along the x-axis in the form of the bar-graph shown in Figure 7. Inspection of the figure indicates that the resulting strains are shown in pairs of bars. The bar on the left of each pair quantifies the response of the dent as-formed on a pipeline pressurized to 0.8 P_{SMYS}. The adjacent bar to its right quantifies the maximum strain after the dent has reshaped in response to re-rounding to a pressure equal to 0.8 P_{SMYS}.

[3] Review of the CEPA[36,37] / PRCI FE dent database[e.g.,see18, Table 1)] and PRCI full-scale test matrix[e.g.,see18, Table 2)] indicates that a limited number of FE models and tests were done at a 45°-angle and a 90°-angle (transverse) to the pipe's long axis using a cylindrical bar indenter. Other skew angles had not been reported at the time the RP was released. Against this limited background database the origins of a criterion that discriminates acceptance at a 30° skew angle is unclear as it is not evident in the matrices reported for their full-scale tests and numerical modeling. Although not considered herein, the same scenario exists for multipeak dents, as a clear path to its criterion is also absent from their matrices.

https://doi.org/10.52202/072781-0004

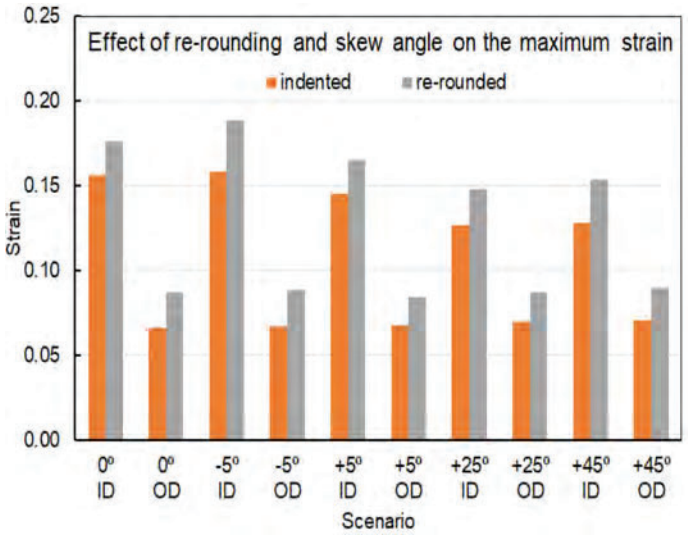

Figure 7. Trends in the maximum strain with skew angle and the effect of re-rounding[after (11)]

Study of the trends in Figure 7 shows that in spite of the very different skew angles considered, the values of the maximum strains formed on both the ID and the OD surfaces for this dent-pipe combination did not show a significant consistent trend with increasing skew angle. While not shown here, it is clear from the corresponding contact-pressure footprints that rotating the contact (skew) angle did not appreciably alter the shape and intensity of their contact pressure distributions. Rather those distributions were similar to that for the 0° case, except for the extent of their rotation. Absent a significant change in the contact-pressure distributions, the strain distributions and intensities remain comparable — so the peak strains remain similar. It is noteworthy that the contact pressure distributions show that these dents were fully unloaded over an area of about 15 square-inches. It is also worth noting that full unloading was evident at dent depths as small as 1% OD. Moreover, the location of the maximum strain in these dents had begun to migrate away from the apex at dent depths as small as 1% OD.

An Issue and Related Observations for Later Discussion

While further study might prove instructive, it is apparent that at the time the RP was released the FEA and full-scale-test databases lacked the scope to establish even tentative recommendations for the effects of skew-angle. This taken with the observation that the values of the maximum strain in regard to Figure 7 did not show a consistent trend with increasing skew angle for the set of very different skew angles considered indicates that the current criterion of the RP is questionable at best, and that the current acceptance of skew angles < 30° appears prone to err significantly.

Discussion

Detailed truth-testing of six of the key assumptions embedded in API RP 1183 has in each case identified an issue with its related practices and closed by noting questions, and/or implications and observations for later consideration in this section. Of these, the questions posed in reference to the first-four assumptions are germane to the implications and/or observations noted for each of the remaining assumptions. For this reason, these overarching questions and their answers are considered first, after which the remaining issues and implications or observations are discussed.

https://doi.org/10.52202/072781-0004

The First Question, and the Apparently Lost Significance of Mesh Refinement

The first question posed in the context of Assumptions 1 to 4 was "can two FEA runs made on comparable commercial platforms solving the same problem using comparable formulations generate fundamentally different answers? — which was answered "YES!" when this question was posed. While there are several plausible reasons for this disconcerting outcome, it suffices here to consider the most probable candidate relative to the PRCI and CEPA reporting[e.g.,24,36,37] that underlie API RP 1183, which is mesh refinement.

The practical significance of mesh refinement becomes clear by reference to books and papers involving the use of FEA, wherein the convergence criteria[e.g., see 38] that establish the worst-case outcome for the problem were often illustrated or discussed as a function of the mesh and element size[e.g.,39]. Against that historical background, the radii of curvature corresponding to the range of dent shapes and sizes listed in Tables 1 and 2 of PRCI's report for its Project MD-5-2[18] were assessed relative to the element sizes used. Its stated use of models reliant on rather coarse element sizes at 2 mm to 4 mm opened to the possibility that the element sizes used were too coarse. This led to truth-testing concerning the viability of those element sizes specific to their use of ANSYS and its 8-node shell element 281[18] (the foundation for the PRCI analyses and that reporting to CEPA[e.g.,36,37]). Head-to-head comparisons[11] showed that mesh refinement in the ANSYS framework led to the same outcome evident for Abaqus making use of its S4 shell element within its refined mesh, which underlies each of References 10 to 13. It suffices in this context to consider the practical significance of mesh refinement as detailed in Figure 8, which has been adapted from Reference 11.

Figure 8 presents the equivalent plastic strain distribution as a function of the element size for an 8-inch diameter D/t = 26 X52 pipe in contact with a rigid 7-inch diameter hemispherical indenter impressed to just 0.6% of the pipe's OD, or 0.052 inch. As usual, the mesh refinement is focused around the zone affected by the contact, and coarsens gradually beyond that area. Seven element sizes were considered within the refined zone, from a maximum of 4 mm (0.157 inch) down to 0.1 mm (0.0039 inch). As indicated above, the coarser among these element-sizes reflect the response that underlies API RP 1183. As the label in the image indicates, these strain distributions were developed for a very shallow dent. This shallow depth was chosen because as the dent deepens the strains intensify in the vicinity of the contact between the pipe and the indenter. As the depth increases the deformations tend to localize such that deeper dents could require still more refined meshes, making deeper dents a potentially worse-outcome as compared to the results presented.

https://doi.org/10.52202/072781-0004

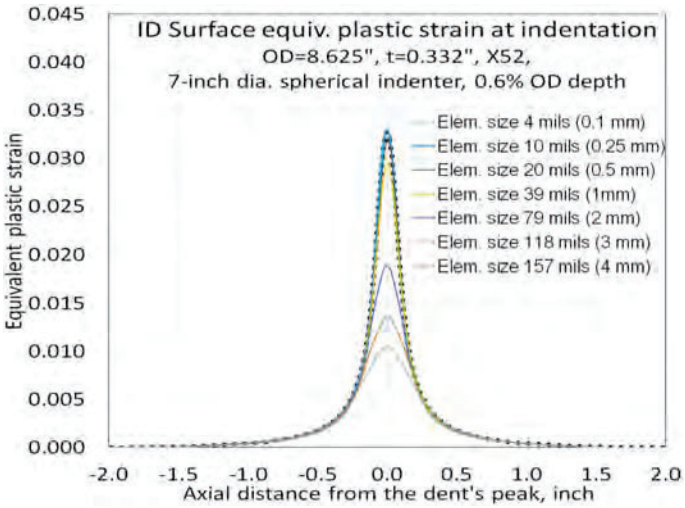

Figure 8. Effect of mesh refinement on the strain distribution within a shallow dent[11]

How or why two FEA runs made on comparable commercial platforms solving the same problem using comparable formulations can generate fundamentally different answers is clearly evident from the trends in Figure 8. For example, the coarsest of the element sizes used in the PRCI modeling (4 mm) leads to a maximum dent strain of 1.05%, while that for the smallest element size (2 mm) used in their reporting leads to 1.90%. In contrast, the maximum strain found via sequential mesh refinement (which was terminated at a two decimal-point change in strain) was 0.0319 or 3.19%. Benchmarked against this maximum strain, the result developed for the 4 mm (0.157 inch) element was unconservative and erred by –67%, while that for the 2 mm (0.079 inch) element erred by –40%. The only way to avoid such disparities is by refining the element-size until the peak strain becomes independent of element size, which because the location of the maximum strain can migrate should be done for each dent-pipe combination.

The Second Question: Significance of Apex Unloading in Regard to 'Restraint'

If unloading occurs leading to zero contact pressure, as was clearly evident in Figure 2, and/or a gap has formed between the indenter and the pipe wall as in Figure 3, then the indenter is not in physical contact with the pipe wall. This observation begs the question: absent physical pipe-to-indenter contact, how can an indenter left impressed at its deepest point 'restrain' the dent's apex — in a full-scale test or in a FEA? In this context is a 'restrained dent' as quantified in API RP 1183 and the underlying PRCI reporting a viable concept? As these questions reflect the same issue noted in the closure to Assumption 9 concerning restraint, suffice it to consider this topic by addressing these questions, as follows.

Logic dictates that the dent's apex cannot be immobilized absent physical contact. This observation coupled with the occurrence of complete unloading even for rather-shallow fully symmetric spherical dents[11] indicates that state of 'restraint' as imposed in the PRCI's FEA and/or full-scale tests by leaving the indenter in place ranges from zero on through some unknown level. Evidence indicative of limited 'restraint' exists in the form of imaging like that replicated here in Figure 9.

https://doi.org/10.52202/072781-0004

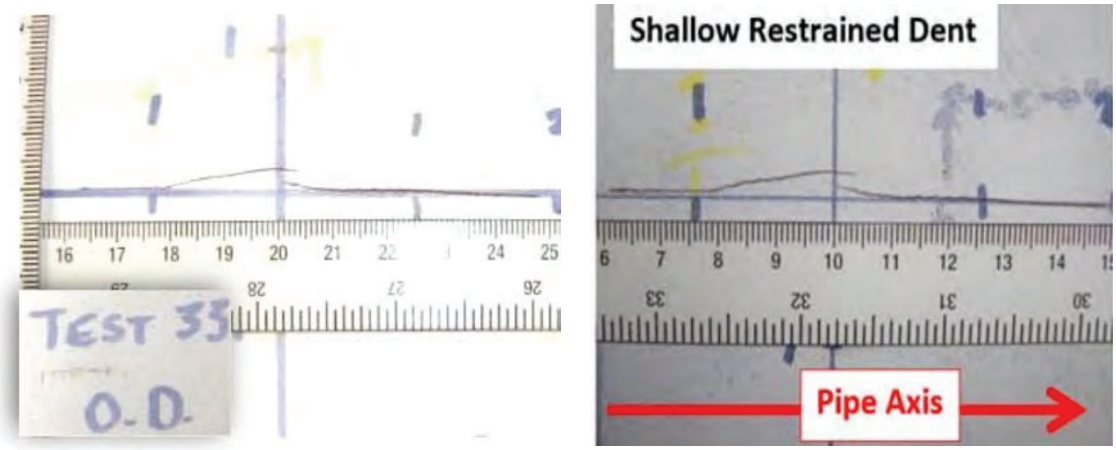

Figure 9. Location and orientation of fatigue crack for shallow restrained dents[1,23]

The left image in Figure 9 is replicated from PRCI Project Report MD-4-14[23], which to the right in this figure appears reimaged and annotated as introduced in Annex B of the RP[1]. The inset into the report's image shown here was cropped from the margin of the original photograph, and included here to document the specific test involved. According to the PRCI reporting[23], Test 33 considered a 'restrained' dent that was formed by a large (24-inch) semi-elliptical indenter impressed to a depth of just 1% OD into a 20-inch diameter X52 pipe with a 0.281-inch-thick wall. This figure illustrates fatigue cracking that initiated and continued to grow in this PRCI full-scale test of a 'restrained' dent. Annex B in the RP notes that this cracking lay at the "center of the dent", which for this image is the intersection of the 'crosshairs' evident in this image. Related imaging of its fracture surface and of cross-sections through this cracking appear consistent with its developing due to fatigue.[23]

Fatigue crack initiation and its continued growth reflect the role of cyclic reversed plastic strain[40]. That said, 'physically immobilizing' (restraining) the dent's apex due to conformal contact with the still impressed indenter precludes local flexure. In addition, the membrane strains developed in a shallow 1% OD dent are minimal. Absent a viable source of cyclic straining, what then drives this fatigue cracking? In response to this question the only plausible driver for fatigue is cyclic flexure made possible because the dent's apex was not immobilized, but rather had unloaded. It is noteworthy that several of the 'restrained' dents detailed in PRCI Report MD-4-14[23] show such cracking near the center of the dent. In contrast, others among the several 'restrained' dents tested developed much different cracking patterns. Plausible reasons for fatigue cracking that initiates near the annulus of contact away from the dent's unloading apex versus remote to it are considered in detail in Reference 12.

The Second Question: Apex Unloading and the Migrating Location of the Maximum Strain

A second equally critical aspect associated with the unloading of a dent's apex is that it occurs in conjunction with the redistribution of the stresses and strains that drives the local reshaping of the dent as the contact patch migrates. In turn, in many cases this affects the migration of the location of the maximum equivalent plastic strain away from a dent's apex. Such migration was evident in fully symmetric dents as well as asymmetric dents at depths as shallow as 1% OD. More importantly, as the migration took the maximum strain inches away from its apex, the strain at the apex no longer reasonably quantified the dent's maximum strains. If the apex strain were taken as the benchmark worst-case strain, as is done within the practices of API RP 1183, then unconservative errors in excess of several hundred percent have been evident[11]. The downside is that no "fix" exists or could be

https://doi.org/10.52202/072781-0004

developed to offset this error in the framework of the RP. On this basis, the utility of the RP's practices is jeopardized at dent depths of a few percent, so the only recourse is to limit the use of API RP 1183 to dent strains or depths below which unloading is no longer a major concern.

The Remaining Issues and Implications – Assumptions 1 to 4, 12, and 13

Oher issues and observations were deferred for later discussion specific to Assumptions 1 to 4, and Assumptions 12 and 13, which are considered here in that sequence.

Assumptions 1 to 4: the Fundamental Basis for API RP 1183 Can Lead to Significant Errors
Whereas the pair of dent-pipe combinations considered in Figure 2 served to highlight issues with the first four assumptions, the disparities discussed were minor except in regard to unloading at the dent's apex. This subsection briefly illustrates a few scenarios for which major disparities emerge concerning the first four assumptions, which are the foundation for API RP 1183. As becomes evident, these major disparities unfortunately can occur in shallow commonly encountered dent-types. As the details are published independently[10,11], this discussion focuses on the results as compared to that based on the RP, which are shown in Figure 10.

As was done in reference to Figure 5, the benchmark for these comparisons is the FEA-determined equivalent plastic strain, and the error is quantified as the difference between the benchmark and the predicted values divided by the benchmark. Figure 10 graphically quantifies 'representative' errors as a function of dent depth, where 'representative' denotes neither the smallest nor the largest error-range within a dataset across all dent-pipe combinations considered. For this reason, the same two dent-pipe combinations considered in Figure 5 are also considered here, with companion data again presented for the OD and ID of the pipe.

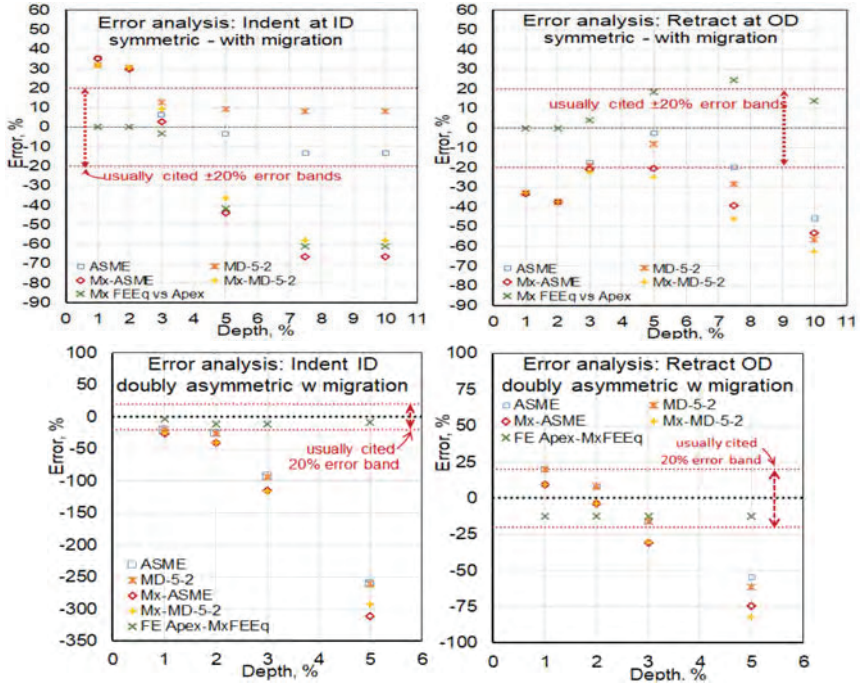

Figure 10. Error analysis considering profile-based effective strains

This error analysis considers the profile-based effective strain as defined in ASME B31.8 Appendix R[17] and the corresponding result for the empirically adapted effective strain as

https://doi.org/10.52202/072781-0004

defined in PRCI Project MD-5-2[18]. By their definitions, these effective strains exist only at the apex of a dent. Errors relative to the FEA apex strain are respectively labeled ASME and MD-5-2. If the location of the maximum strain migrated away from the single-peak apex, the resulting error relative to the FEA maximum dent strain is respectively labeled Mx ASME or Mx MD-5-2. In such cases, the error in the use of the FEA Apex versus the FE Maximum strain is denoted FE MxFEEq–FE Apex. All images include the ±20% error bounds commonly shown in PRCI MD-5-2 Project report.

Study of the trends in the upper left image in Figure 10 shows that at small dent depths and correspondingly small strains there is little difference in the values of the ASME and the MD-5-2 effective strains. This was the case across the many cases evaluated. At these shallow dent depths these effective strains err conservatively by about 17%. At depths above of 2% OD their values relative to the FE apex begin to diverge, but in all cases their values remain within the ±20% error bounds. At depths above of 3% OD their values as compared to the strain at the now migrating location of the maximum equivalent plastic strain begin to diverge from that at the apex. As the location of the maximum equivalent plastic strain migrates from the apex, the unconservative error developed by the ASME and the MD-5-2 effective (apex) strains relative to the maximum value of the FE equivalent plastic strain (i.e., with the prefix Mx) becomes larger. As the figure shows their values track along with the error trend shown for FE MxFEEq–FE Apex. It is apparent for this dent-pipe combination that the unconservative error associated with the profile-based effective strains becoming significantly nonconservative at depths deeper than 4% OD, which by 6% OD are approaching –80% relative to the FE benchmark maximum strain. Errors of this magnitude completely erode the design margin even for operations at the lowest allowable design stress for transmission pipelines.

Because the strain distributions on the ID and OD surfaces differ due to the contact being focused on the OD, the error analysis leads to quite different trends on the OD surface. Even so, study of the upper-left image indicates that the outcomes are similar. The errors for the profile-based effective strains relative to the FE benchmark at the site of the migrating maximum strain in this case approach –60% relative to the FE benchmark maximum strain. Errors of this magnitude likewise erode the design margin for transmission pipelines operating in high-consequence / unusually sensitive areas.

In many ways the error trends for the lower-pair of images shown in Figure 10 are comparable to that just considered — except that for this dent-pipe combination the onset of migration occurred at somewhat a shallower depth (about 1% OD), and that the worst-case unconservative error in the profile-based effective strains exceeded –200%. It is left to the reader to delve into the details of these plots to the extent they care to.

Suffice it here to note that no "fix" exists or could be developed to offset such errors in the framework of the RP, as its approach is: 1) coupled to profile-based strains set at the dent's apex; and 2) insight as to the location of the maximum strain in the dent is not evident from its shape or depth profiles. On this basis, the utility of the RP's practices is jeopardized at dent depths deeper than a few percent, so the only recourse is to limit is used to dent strains or depths below which unloading is no longer a major concern. It follows that prudence dictates caution when using the practices of the RP in applications to asymmetric dents at depths greater than about 1%, whereas 2% appears plausible for symmetric dents based on the results in hand.

Assumption 12: Significant Persistent Scatter Traced to the Shape Parameter

The early trending of the predictions of Eqn. (28) showed that its very scattered outcomes were clearly banded as functions of the imposed constant-amplitude pressure cycling, which reflects the modeling

https://doi.org/10.52202/072781-0004

error embedded in SP as it was initially formulated, and curve-fitted. On this basis, if consistent with Assumption 11 of the RP Eqn. (28) was coupled with a single resistance curve like that in BS 7608[25], then the resulting scatter would be untenable. Two paths existed to minimize the model-error induced scatter to a practically acceptable level: 1) reformulate the SP to eliminate or suitably reduce the sources of the model error; and/or 2) empirically offset the potential sources of its error to a 'manageable' level. Of these, given the strong dependence in scatter on the imposed constant-amplitude pressure cycling conditions[33], it appears that the second option was pursued. Evidently the predictions of N as a function of SP were correlated specific to the datasets developed across the set of constant-amplitude pressure histories used in the PRCI-CEPA FEA, which resulted in the tabulations listed in Annex F of the RP. This Annex presents the outcomes of such a process as a family of constants for use in Eqn. (28) of API RP 1183, the expectation being that this would adequately offset a significant component of the model-error embedded in the formulation of SP.

The benefit affected by the use of the pressure-history specific curve fits now listed in Annex F of API RP 1183 can be established by quantifying the reduction in scatter affected through this empirical 'fix' with the outcomes of the early curve-fitting done circa 2014[33]. That said, head-to-head comparisons between the trends reported in 2014[33] versus that done in 2022[34] shows no apparent difference in the fitting parameters over the intervening 8-year interval. As such, the empirical 'fix' affected by the pressure-history specific curve-fits in Annex F are still associated with a scatter-band for the shape parameter as large as 200-fold (compare Figure 5-10 in Dinovitzer et al[34] with the figures in Annexes E and F in Tiku et al[33]). On this basis, the model-error embedded in the shape parameter still remains very large, such that the lives predicted based on the SP will remain very scattered. More critically, because the curve-fits that underlie Annex F of API RP 1183 reflect the central tendency within the scatter band, some predictions will remain very conservative while others will be equally unconservative. This scatter will persist until the complexity embedded in the dent's deformation history is addressed, and the uncertainty embedded in 'restraint' is resolved.

Unfortunately, the dent's reshaping as it deforms and its contact pressure distribution evolves opens to its apex unloading and its peak strain's migration, which cannot be captured within the approximations that underlie RP 1183 — except at strains below which this behavior occurs. In turn this limits the utility of its practices to rather shallow dents, and even these can be issues. Based on the results in hand[10,11], the apex of a fully symmetric inverse-dome-shaped dent can unload completely at depths as shallow 2% OD. That said, cases where the apex has fully unloaded have occurred at depths as shallow as 1% OD in applications involving large-area low curvature dents[11].

It follows that prudence dictates caution when using the practices of the RP in applications to fully symmetric dents at depths greater than 2%. Recognizing that such unloading confounds the practices of the RP in applications to potentially 'restrained' dents, care is likewise warranted in such scenarios.

Assumption 13: the Questionable Criterion for Skew-Angles Set at ≥ 30°

As Footnote 3 noted, the scope of the CEPA and PRCI FE dent databases and the PRCI full-scale test matrix did not broadly consider the effects of skew-angle. Against this limited scope, the origin of the RP's criterion that discriminates skew-acceptance for Level 2 assessment at a 30° skew angle is unclear, as support for it is not evident in the full-scale tests and numerical modeling that underlie the RP. Although further study might prove instructive, several observations are relevant that include:

1. large strain gradients can develop over very small distances within even shallow dents;
2. the maximum dent-strain did not show a consistent dependence on skew-angle within the set of very different skew angles considered;

https://doi.org/10.52202/072781-0004

3. large predictive errors were evident for the practices of API RP 1183 for dent skew angles as small as ±5°[11]; and
4. results in related publications indicate that the largest strains for skew dents lie along or close to the skew axis [e.g.,41].

These observations taken together support the contention that relatively small skew angles can prove problematic. On this basis, the current acceptance of skew angles < 30° appears prone to err significantly. Whether or not skewed-dents can be safely and reliably assessed at Level 2 remains an open question. It follows that prudence dictates caution when using the practices of the RP in applications to dents skewed to the long axis by more than a few degrees.

Summary, Conclusions, and Takeaways

This paper identified 13 among the key assumptions latent in the Level 1 and Level 2 practices of API RP 1183. Of the 13 identified, eight that are considered central to the current or next revision of the RP were truth-tested by comparison with results generated using full-scale-validated Level 3 analyses. Results for smooth single-peak symmetric and asymmetric dents formed in geometrically stiff versus compliant pipes over a range of depths from less than 1% OD up to 10% OD were considered. Disparities were identified for each that were associated with significant unconservative predictive errors that exceeded –50%, which occasionally approached or exceeded –100%. Key factors driving those errors included the use of coarse elements in the supporting numerical work, and the migration of the contact-patch formed between the pipe wall and the contact (indenter), which leads to unloading at the dent's apex, and the migration of the site of the maximum strain away from the dent's apex. Observations and guidance were presented based on the results in hand concerning the safe use of the RP, which leads to takeaways that follow shortly.

Some high-impact conclusions and takeaways follow that given their implications and consequences could generate both controversy and consternation. That said these conclusions and takeaways reflect a limited body of evidence, whose outcomes are internally consistent across a scope that reflects the bounds and range of dent-pipe combinations evident in Figure 1 — which is cause for pause.

A number of conclusions follow concerning the aspects of dent strain and deformation considered in summary herein, and elsewhere in detail[10,11] including:

- while the maximum FE equivalent plastic strain initially develops at the dent's deepest point, its apex, in response to the migration of the contact-patch formed between the pipe and the indenter as the dent deepens and reshapes, the location of this maximum strain also migrates — in some cases by several inches[10,11];
- because the location of the maximum FE equivalent plastic strain can migrate, the apex-centric practices of API RP 1183 fail to track its migration, and were shown prone to err in that context non-conservatively by –50% — and in some cases erred well beyond –100% even for simple rather shallow fully symmetric dents;
- as the location of the worst-case strain cannot be simply inferred by reference to a dent's deepest point, the simpler Level 1 and Level 2 dent-shape-based practices of the RP cannot be extended, adapted, refined, updated, or empirically made case-specific to manage this migration — the only recourse is to limit use of the PR to strains and related dent-depths below which migration occurs;

https://doi.org/10.52202/072781-0004

- related to the migration of the contact-patch formed between the pipe and the indenter as the dent deepens, it has become evident that this contact is 'conformal' to the indenter only at shallower dent depths the extent to which is dependent on the pipe's stiffness (affected by both internal pressure and *D/t*), whereafter the dent's apex can fully 'unload' to zero interface contact pressure, and a gap can form between the pipe-wall and the indenter;
- physical contact between the apex and the indenter ceases as the contact-pressure drops to zero and a gap forms — how then can an indenter left at its maximum depth affect 'restraint' at the dent's apex, so the extent of 'restraint' as determined by the methods of the RP remains open to question;
- elastic FEA formulations are limited in their ability to quantify migration of the contact patch and its consequences in the form of unloading at the dent's apex, and the migration of the maximum strain away from the apex, and so should be used with caution at dent depths where these processes become active;
- there is little evidence concerning the effects of skew-angle developed in the body of work that underlies the RP to establish its criterion that skew-angles ≤ 30° can be managed using Level 2 methods — the current work shows little influence of skew-angle, while it also shows steep strain gradients develop within dents — because the peak strain lies along the skew-axis rather than the axial dent profile, even low-angle skewed-dents should be assessed at Level 3.

Conclusions relevant to the few aspects involving the fatigue analysis of dents according to the practices of API RP 1183 summarized herein and elsewhere[12] include:

- the large model-error embedded in the shape parameter, SP, early in its formulation circa 2014[33] remains today[see 34], leading in some cases to scatter in the SP by a factor of about 200 for the same predicted life — caution is warranted given that the curve-fitted trends in Annex F of the RP reflect the mean tendency within that scatter-band;
- given that the management of 'restraint' as set forth in the methods of the RP relied on the presumption of conformal contact between the pipe-wall and the indenter, whereas gaps were locally evident in the current work, and fatigue cracking developed in tests within the area of 'restraint', — caution is warranted until the assumed state of restraint is confirmed.

In addition to the above concern remains due to the potentially unconservative role of element size regarding its impact on the quantitative aspects of API RP 1183. This aspect has been considered independently[13].

Important takeaways aside those in the conclusions include:

- the evidence in hand indicates that the analysis approach that underlies RP 1183 opens to large unconservative errors at dent strains > 3%, and its fatigue predictions are prone to scatter;
- other methods like the simpler stress-concentration factor concept[42] have proven useful within this same strain limit[e.g.,43] and so should be given broader consideration;
- as the basic tenants of API RP1183 cannot be made relevant to higher strains, there is cause for pause when assessing the path forward concerning dent management.

https://doi.org/10.52202/072781-0004

References

[1] API Recommended Practice 1183, Assessment and Management of Dents in Pipelines, November, 2020, 1st Errata, January, 2021.

[2] API Website:https://www.api.org/products-and-services/standards/important-standards-announcements/rp1183, accessed 03-20-2023.

[3] Belanger, A. and Burden, D., "Implementing API 1183 in an ILI Survey", Paper 66, 34th International PPIM Conference, Houston, February, 2022.

[4] Bao, J., Zhang, S., Zhang, B., Wang, R., and Zhang, K., "An Automatic Dent Assessment Tool using Finite Element Method", 14th International Pipeline Conference, IPC2022-87098, ASME, Calgary, September 2022

[5] Polasik, S., Wu, S., Bratton, J., Dotson, R., and Sager, R., "The State of Dent Screening and Shape-Based Assessments: Discrepancies to Consider", 14th International Pipeline Conference, IPC2022-87301, ASME, Calgary, September 2022.

[6] Lockey, A., Turner, S., Turner, T., and Kirkwood, M., "Applying API RP 1183 to Real-World In-Line Inspection Dent Data", 35th International Pipeline Pigging and Integrity Management Conference, Houston, February 2023 pp. 63-84.

[7] Hardy, J. and Newton, C., "Detaining Dents – Determining Restraint for Dents Measured by ILI Case Study," 35th International PPIM Conference, Houston, February, 2023, pp 301-322.

[8] Wu, S., Bratton, J., Wang, J., Kemp, K., "192 Final Rule (RIN2) – Essential Elements and Guidelines to Perform a Dent Engineering Critical Assessment", 35th International PPIM Conference, Houston, February, 2023, pp. 277-300.

[9] Bankehsaz, M., Sager, R., Slane, D., "Investigating the Impact of Full-Scale Fatigue Testing and Changes to Formation Strain Predictions on Dent Integrity", 35th International PPIM Conference, Houston, February, 2023, pp. 323-344.

[10] Leis, B.N., Eshraghi, M.A., Dew, B.A., and Cheng, Y.F. "Dent Strain and Stress Analyses and Implications Concerning API-RP 1183 - Part I: Background for Dent Geometry and Strain Analyses During Contact and Re-Rounding, J Pipeline Science & Engineering, December, 2023. https://doi.org/10.1016/j.jpse.2023.100143

[11] Leis, B.N., Eshraghi, M.A., Dew, B.A., and Cheng, Y.F. "Dent Strain and Stress Analyses and Implications Concerning API-RP 1183 - Part II: Examples of Dent Geometry and Strain Analyses During Contact and Re-Rounding, J Pipeline Science & Engineering, in press, 2023

[12] Leis, B.N., Eshraghi, M.A., Dew, B.A., and Cheng, Y.F. "Dent Strain and Stress Analyses and Implications Concerning API-RP 1183 - Part III: Cyclic Loading and Fatigue-Life Prediction, J Pipeline Science & Engineering, soon in press, 2023

[13] Leis, B.N., Eshraghi, M.A., Dew, B.A., and Cheng, Y.F. "Dent Strain and Stress Analyses and Implications Concerning API-RP 1183 - Part IV: Mechanics and Modeling Aspects of Dent Strain and Fatigue Analyses for Contact and Re-Rounding and In-Service Loadings, J Pipeline Science & Engineering, in draft, 2023

[14] Singh, A., Langer, D., Woo, J., Yoosef-Ghodsi, N., Kainat, M., "Improved Semi-Quantitative Reliability-Based Method for Assessment of Pipeline Dents with Stress Risers", 13th International Pipeline Conference, IPC2020-9472, ASME, Calgary/Virtual, September 2020.

[15] Zhang, S, Zhang, B., and Wang, R., "A Transparent ASME B31.8-Based Strain Assessment Method using 3D Measurement of Dent Morphology", 14th International Pipeline Conference, IPC2022-, ASME, Calgary/Virtual, September, 2020.

[16] Gao, M., Krishnamurthy, R., and Wang, R., "A Newly Improved Fatigue Life Prediction Model for Unconstrained Single Peak Plain Dents Based on EPRG Approach," Draft for Review to J Pipeline Science and Engineering, Accessed 11-24-2023.

[17] ASME B31.8, "Gas Transmission and Distribution Piping Systems," 2020.

[18] Rana, A., Tiku, S., and Dinovitzer, A., "Improve Dent/Cracking Assessment Methods," Catalog PR-214-203806-R01, PRCI Project MD-5-2, 2022.

[19] Gao, M., McNealy, R., Krishnamurthy, R., and Colquhoun, I., "Critical Strain Based Ductile Damage Criterion and its Application to Mechanical Damage in Pipelines," 7th International Pipeline Conference, Calgary, IPC 64565, ASME, 2008.

[20] Leis, B.N., Nelson, D.V., and Socie, D.F., "Fatigue Life Prediction", Chapter 10 in Fatigue Design Handbook, 2nd Edition, Society of Automotive Engineers, R. C. Rice, B. N. Leis, and D. V. Nelson Editors, 1989.

[21] Tiku, S., Semiga, V., Dinovitzer, A., and John, B., "Full Scale Fatigue Testing of Dents (Plain and Interacting with Welds and Metal Loss)," Catalog PR-214-073510-R01, PRCI Project MD-4-2, 2018.

[22] Tiku, S., Eshraghi, A., John, B., Dinovitzer, A., Zarea, M., Fernandez, C., and Bertin, M., "Full Scale Testing of Interactive Features for Improved Models", PHMSA DTPH56-14-H-000024-11 / PRCI Project MD-4-11, September, 2017.

[23] Tiku, S., Eshraghi, A., John, B., and Dinovitzer, A., "Full-Scale Testing of Shallow Dents with and without Interacting Features", Catalog PR-214-163714-R01, PRCI Project MD-4-14, October, 2019.

[24] Tiku, S., Eshraghi, A., Rana, A., and Dinovitzer, A., "Fatigue Life Assessment of Dents with and without Interacting Features", Catalog PR-214-114500, PRCI Project MD-4-9, 2018.

[25] Anon., "Guide to Fatigue Design and Assessment of Steel Products", BS 7608 circa 2008.

[26] Maddox, S.J., The Fatigue Strength of Welded Structures, 2nd Ed., Abington Publishing, Cambridge, 1991.

[27] MacDonald, K.A., Maddox, S.J., and Haagensen, P.J., "Guidance for Fatigue Design and Assessment of Pipeline Girth Welds", UK Health and Safety Executive Report OTO 2000 043, 2000.

[28] Karabayrak, B., Baskut, S., and Turan, D., "Investigation of the Mechanical Properties of Calcium Treated Low Carbon Steel", Arch. Metall. Mater., Vol. 68, 2023, pp. 89-96: DOI; doi.org/10.24425/amm.2023.141478.

[29] Hohl, G., "Resistance of Gas Transmission Pipelines to Mechanical Damage and Failure - Analysis of EPRG Test Results, Part I: Test Results", MFI-Report UB 114/91,1991, and "Part II: Critical Damage and Failure Criteria", MFI-Report UB 2/92, 1992.

[30] Basquin, O.H., "The Exponential Law of Endurance Test", Proceedings, American Society for Testing and Materials", Vol. 10, 1910, pp. 625-630.

[31] Morrow, J.D., "Cyclic Plastic Strain Energy and Fatigue of Metals", in Internal Friction, Damping and Cyclic Plasticity, ASTM STP 378, 1965, pp. 45-87.

[32] CSA Z662:19, "Oil and Gas Pipeline Systems", CSA Group, 2019.

[33] Tiku, S., Eshraghi, A., Semiga, V., and Dinovitzer, A. "Technical Note: Dent Fatigue Life Assessment and Dent Weld Interaction", BMT 6837B-TN001, Draft Interim Report, PRCI Project MD 4-9, May, 2014.

[34] Dinovitzer, A., Leis, B., Krishnamurthy, R., Alexander, C., and Zarea, M., "Systematize 20 Years of Mechanical Damage Research", Catalog PR214-203804-R01, PRCI Project MD-5-1, May, 2022.

[35] Grover, H.J., Gordon, S.A., and Jackson, L.R., Fatigue of Metals and Structures, Bureau of Naval Weapons, US Department of the Navy, NAVWEPS 00-25-534, 1954, Rev 1, 1960.

[36] Eshraghi, A., Tiku, S., Rana, A., "Management of Shallow Restrained Dents", Technical Report to the Canadian Energy Pipeline Association (CEPA), Report. No. 30620-RPT01 (Rev. 02), 2018.

[37] Eshraghi, A., Tiku, S., Rana, A., "Management of Unrestrained Dents", Technical Report to CEPA, Report. No. 30724-RPT01 (Rev. 01), 2019.

[38] Zienkiewicz. O.C., The Finite Element Method in Engineering Science, McGraw-Hill, 1971 (see §3.2 Convergence).

[39] Stonesifer, R. B., Brust, F. W., and Leis, B. N., "Mixed Mode Stress Intensity Factors for Interacting Semi-Elliptical Surface Cracks in a Plate", Eng. Fracture Mech., Vol. 45, No. 3, 1993, pp. 357-380.

https://doi.org/10.52202/072781-0004

[40] Klesnil, M. and Lukas, P., Fatigue of Metallic Materials, Elsevier, 1980.

[41] Leis, B. N., Forte, T. P., and Zhu, X-K, "Integrity Analysis for Dents in Pipelines", 5th International Pipeline Conference, ASME IPC04-0061, ASME, Calgary, 2004.

[42] Fowler, J.R., Alexander, C.R., Kovach, P.J., and Connelly, L.M., "Cyclic Pressure Fatigue Life of Pipelines with Plain Dents, Dents with Gouges, and Dents with Welds", PRCI Reports PR201-927 1992 and PR201-9324, 1994: see also Paper 15, 10th EPRG-PRCI JTM, Cambridge, 1995.

[43] Dotson, R., Holliday, C., Torres, L., and Hagan, D., "An Authoritative Comparison of Remaining Life Assessments for Pipeline Dents", 12th International Pipeline Conference, September, 2018, Calgary, IPC2018-78247 – and private communications with its first author, October 2023.

https://doi.org/10.52202/072781-0004